Light illumination effect on the electrical and photovoltaic properties of In_6S_7 crystals

2006 J. Phys.: Condens. Matter 18 4609

(http://iopscience.iop.org/0953-8984/18/19/014)

INSTITUTE OF PHYSICS PUBLISHING JOURNAL OF PHYSICS: CONDENSED MATTER

J. Phys.: Condens. Matter **18** (2006) 4609–4614 doi:10.1088/0953-8984/18/19/014

Light illumination effect on the electrical and photovoltaic properties of In_6S_7 crystals

A F Qasrawi[1,3] **and N M Gasanly**[2]

[1] Department of Electrical and Electronics Engineering, Atilim University, Kizilcasar Koyu, Incek, Golbasi, Ankara 06836, Turkey
[2] Department of Physics, Middle East Technical University, Ankara 06531, Turkey

E-mail: atef_qasrawi@atilim.edu.tr

Received 3 February 2006
Published 26 April 2006
Online at stacks.iop.org/JPhysCM/18/4609

Abstract

The electrical and photoelectrical properties of In_6S_7 crystals have been investigated in the temperature regions of 170–300 K and 150–300 K, respectively. The dark electrical analysis revealed the intrinsic type of conduction. The energy band gap obtained from the temperature-dependent dark current is found to be 0.75 eV. It is observed that the photocurrent increases in the temperature range of 150 K up to $T_m = 230$ K and decreases at $T > T_m$. Two photoconductivity activation energies of 0.21 and 0.10 eV were determined for the temperature ranges below and above T_m, respectively. The photocurrent (I_{ph})–illumination intensity (F) dependence follows the law $I_{ph} \propto F^{\gamma}$. The value of γ decreases when the temperature is raised to T_m, then it starts increasing. The change in the value γ with temperature is attributed to the exchange in role between the recombination and trapping centres in the crystal. The crystals are found to exhibit photovoltaic properties. The photovoltage is recorded as a function of illumination intensity at room temperature. The maximum open-circuit voltage and short-circuit photocurrent density, which are related to an illumination intensity equivalent to one sun, are 0.12 V and 0.38 mA cm^{-2}, respectively.

1. Introduction

The compound In_6S_7 is a semiconductor which crystallizes in a monoclinic structure. The crystal structure consists basically of two separate sections, both consisting of almost cubic close-packed arrays of S atoms with In atoms in octahedral coordination, the two sections having equivalent directions at 61.5° to each other. The crystalline phase of this compound has been obtained by two growth techniques: the Bridgman technique [1–5] and the so-called travelling heater method [6].

[3] Author to whom any correspondence should be addressed.

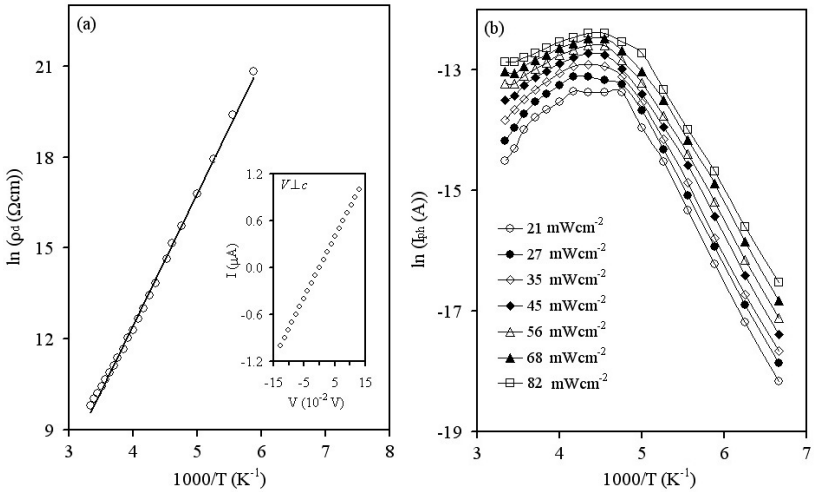

Figure 1. (a) Variation of $\ln(\rho_d)$–T^{-1} for In_6S_7 crystals. Inset: I–V characteristic. (b) The $\ln(I_{ph})$–T^{-1} dependence.

Literature concerning the preparation and physical properties of In_6S_7 crystal is relatively rare due to the difficulty of growing large single crystals. Some of the physical properties of this compound have been investigated. In particular, temperature-dependent photoelectric spectra [1], infrared spectra [3, 4], the temperature-dependent absorption band edge [5], thermoelectric power and conduction mechanism [6] have been studied. In spite of the above-reported studies, literature still lacks information about the physical interpretation of the temperature-dependent dark and photoconduction properties. The purpose of this work is to report these properties for the Bridgman-technique-grown In_6S_7 single crystals. In addition, the observation of the photovoltaic effect in In_6S_7 crystals will be reported and discussed.

2. Experimental details

In_6S_7 polycrystals were synthesized from high-purity elements (at least 99.999%) taken in stoichiometric properties. The single crystals were grown by the Bridgman method. The x-ray diffraction patterns show that these crystals have a monoclinic structure with the lattice parameters $a = 0.909, b = 0.389, c = 1.771$ nm and $\beta = 108.20°$. The resulting single-crystal layers were not subjected to any additional annealing. Typical dimensions of the crystals suitable for measurements were $5 \times 5 \times 3$ mm^3. Using silver paste, four-point contacts were fixed at the top surface of the sample. The ohmic nature of the contacts was confirmed by the I–V characteristics displayed in the inset of figure 1(a). The I–V characteristics recorded perpendicular to the crystal c-axis are found to be linear and independent of the reversal current for low applied voltages ($V < 0.2$ V). Cooling of the sample was achieved by means of a closed-cycle cryostat (Advanced Research Systems) and Lake Shore 340 temperature controller. The dark electrical resistivity and photocurrent were measured using a dc Keithley 6430 SUB-FEMTOAMP remote source/electrometer. The dark electrical resistivity measurements were made by the Van der Pauw technique. The resistivity and photocurrent measurements were made under a bias voltage of 0.10 V (ohmic region). Illumination was provided by a halogen lamp. The light intensity was calibrated using an IL 1700 radiometer.

3. Results and discussion

To establish the dominant transport mechanism and identify the impurity levels in the In_6S_7 crystals, the temperature dependence of the dark electrical resistivity (ρ_d) was measured in the temperature range of 170–300 K. A general view of the dark resistivity as a function of reciprocal temperature is displayed in figure 1(a). It is clear from the figure that ρ_d systematically increases upon temperature lowering. The measured data of ρ_d–T dependence is found to follow the relation,

$$\rho_d = \rho_0 \exp\left(-\frac{E_g}{2kT}\right), \tag{1}$$

where ρ_0 is the pre-exponential factor and E_g is the energy band gap of the crystal. This equation was used because the crystals are known to exhibit intrinsic n-type conduction [6] in this temperature range. According to equation (1), the slope of the $\ln(\rho_d)$–T^{-1} graph (the solid line in figure 1(a)) reveals an energy band gap of 0.75 eV. The obtained band gap confirms the fact that In_6S_7 crystals exhibit intrinsic-type conduction and agrees with the optically determined band gap being 0.7 eV at room temperature [5].

It is worth noting that the fitting procedure was carried out by a special high-convergence minimization program that makes use of regression and residual sums of squares (R^2), the coefficient of determination, and the residual mean squares statistical analysis. The errors in the data were evaluated to be 2–10%. The typical best fit for the experimental data is illustrated by the solid line in figure 1(a). The calculated slope was restricted to give a residual sum of squares $R^2 > 0.99$.

Photocurrent (I_{ph}) measurements were carried out at different light intensities (F) in the range of 21–82 mW cm^{-2}. The bias voltage was fixed at 0.10 V. Illumination was provided by a halogen lamp and filtered by using discrete filters. The incident light was restricted to allow transitions at a wavelength of (1600 ± 50) nm. The photosensitivity, S, defined as I_{ph}/I_d, is found to increase with increasing illumination intensity and decreasing temperature. For example, the crystal exhibits photosensitivity of 0.2, 0.5 and 0.9 at 300 K, which increases to 3.0×10^2, 5.4×10^2 and 1.0×10^3 at 200 K and reaches 3.4×10^3, 7.6×10^3 and 1.8×10^4 at 150 K for applied illumination intensities of 21, 45 and 82 mW cm^{-2}, respectively.

Figure 1(b) shows representative data of the experimental photocurrent as a function of reciprocal temperature for In_6S_7 crystals at different illumination intensities. The figure illustrates the exponential increment in photocurrent with temperature increase in the range of 150 K $\leqslant T < T_m$, where $T_m \sim 230$ K is the temperature corresponding to the maximum photocurrent value. In the temperature range where $T > T_m$, the photocurrent decreases steeply with an increase in T. It is clear from figure 1(b) that plots of $\ln(I_{ph})$–T^{-1} consist of two distinct regions. In the first temperature region, 150 K $\leqslant T < T_m$, the exponential increase in photocurrent with temperature in accordance with the expression $I_{ph} \propto \exp(-E_{ph}/kT)$ displays photocurrent activation energy $E_{ph1} = 0.21$ eV. In the second region, $T > T_m$, the exponential decrease in photocurrent with temperature according to the relation $I_{ph} \propto \exp(E_{ph}/kT)$ reveals an average photocurrent activation energy of $E_{ph2} = 0.10$ eV.

On the other hand, figure 2(a) illustrates a typical representation of the photocurrent growth as a function of illumination intensity at different temperatures. As is clear from the figure, $I_{ph} \propto F^{\gamma}$. Generally, γ is observed to vary upon temperature change. The variation of γ with temperature is displayed in figure 2(b). As can be detected from this figure, γ decreases from 1.22 at 300 K to 0.65 at 240 K and increases again with temperature decrement. The behaviour is consistent with that of I_{ph}–T dependence. Particularly, in the region 150 K $\leqslant T < T_m$, γ decreases as temperature increases (from 1.12 at 150 K to 0.63 at 220 K). In the region $T > T_m$, γ rises with increasing temperature. In other words, in the region where $E_{ph1} = 0.21$ eV is

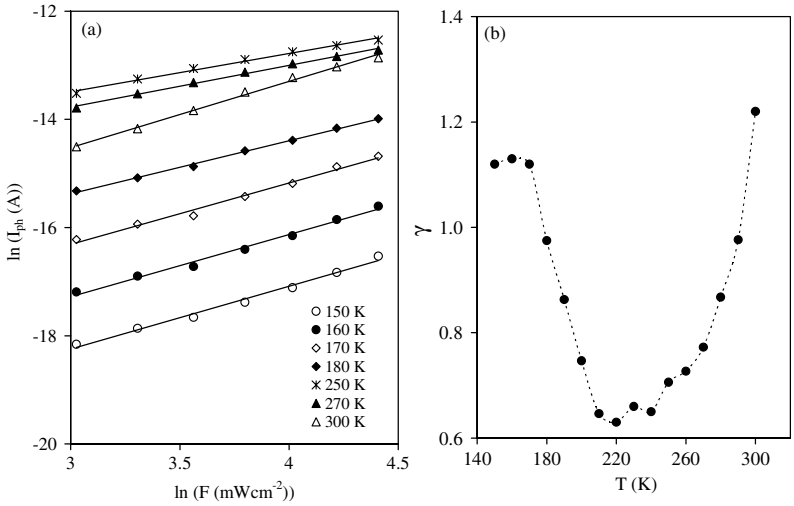

Figure 2. (a) The I_{ph}–F dependence at various temperatures for In_6S_7 crystals. (b) The γ–T dependence. The dashed curve is only a guide for the eye.

active, γ decreases and, in the region where $E_{ph2} = 0.10$ eV is dominant, γ increases with temperature.

The change in the values of γ with temperature could be explained by the recombination model with an exponential trap distribution [7]. The model suggests that changes in the position of the dark Fermi level may be much more important than the related changes in defect densities in these cases: one-to-one correlation between defect density and photoconductivity may not be observed. The changes in the density of trapping states caused by illumination shift the position of the Fermi level. The model suggests the validity of the relation $I_{ph} \propto F^{\gamma}$ and defines the value of γ as

$$\gamma = \frac{T^*}{T^* + T}, \tag{2}$$

where T^* is a parameter describing the exponential trap distribution. When the carriers are trapped, they are unable to participate in the dynamical recombination process. This effect tends to depopulate deep recombination centres, making more of them effective in reducing the carrier lifetime. Equation (2) shows that: at $T^* \gg T$, γ tends to unity and all the recombination centres are empty; at $T^* = T$, γ is equal to 0.5 and the density of carries trapped below the Fermi level is less than the density of carriers trapped above the Fermi level. For the case $T^* \geqslant T$, equation (2) indicates that $0.5 \leqslant \gamma \leqslant 1$ and the density of empty recombination centres varies with excitation rate as a result of a near equality of densities of trapped carriers, and empty recombination centres both being larger than the free carrier density.

Similar behaviour of temperature-dependent photocurrent was also observed in $GaSe_{0.95}S_{0.05}$:Na mixed crystals [8] and $TlInS_2$ crystals [9]. For these crystals, the photocurrents were also observed to increase with increasing temperature up to critical temperatures of 357 and 245 K, respectively. Above this temperature, I_{ph} decreases with increasing temperature. This type of variation in I_{ph} with temperature was explained in terms of the above-reported model [7] (i.e. assuming the existence of deep recombination centres and shallow traps). These levels are electron trapping levels located at E_{ct} below the conduction band and hole trapping levels located at E_{vt} above the valence band. The levels are assumed to be in quasi-equilibrium with the corresponding band. In accordance with the model, the

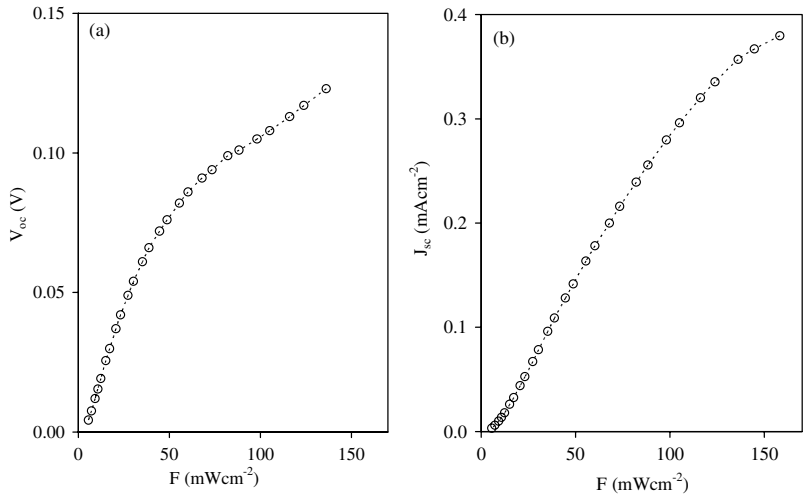

Figure 3. (a) The V_{oc}–F dependence for In_6S_7 crystals recorded at 300 K. (b) The J_{sc}–F plot. The dashed curves are only a guide for the eye.

I_{ph}–T variation in In_6S_7 crystal could be explained as follows: at fixed illumination intensity with increasing temperature, the maximum temperature T_m is reached at which the minority carriers (holes) are thermally reactivated from their trapping level into the extended valence band, providing additional free holes. Therefore, these free holes are easily captured in deep recombination centres, where they recombine with free electrons. Hence, the lifetime of the majorities carriers (electrons) is shortened, leading to a decrease in the photocurrent, as observed in figure 1(b).

Figures 3(a) and (b) display the linear open-circuit photovoltage response (V_{oc}) and the related short-circuit current density (J_{sc}) as a function of illumination intensity—being recorded under zero bias voltage conditions—at 300 K, respectively. The data were recorded parallel to c-axis of the crystal. A systematic increase in V_{oc} and J_{sc} is observed upon an increment in F. The behaviour is an indication of the photovoltaic property. For low applied F ($5 \leqslant F \leqslant 35$ mW cm^{-2}), J_{sc} is observed to exhibit supralinear character ($\gamma = 1.9$); in the region of $35 \leqslant F \leqslant 90$ mW cm^{-2}, the I_{sc}–F variation is linear ($\gamma = 1.0$); and above 90 mW cm^{-2}, γ is found to be 0.7. The maximum photovoltage, obtained at an illumination intensity of 137 mW cm^{-2} (1.0 sun), is equal to 0.12 V. The corresponding short-circuit current density is 0.38 mA cm^{-2}. These values are comparable to that reported for ZnO/CdTe/CuSCN *eta*-solar cells [10], and CIS/IS/ZnO and CIS/CdS/ZnO solar cells [11]. These features of In_6S_7 crystals are promising characteristics for the usage of In_6S_7 crystals for solar cell fabrication.

In an attempt to explain the appearance of supralinear characteristics in the photocurrent–illumination intensity dependence at fixed temperatures, we recall that the recombination model with exponential trap distribution presented by equation (2) terminates. The supralinear phenomena can be explained by means of two recombination centres. Namely, when two recombination centres below the Fermi level are optically excited, the interaction between these centres gives rise to supralinear photoconductivity. In other words, when the sensitizing centres (trapping centres) behave like recombination centres, the electrons present in the sensitizing centres are effectively transferred to the recombination centres (if the density of the recombination and sensitizing centres is much larger than the density of free carriers), thereby decreasing the density of empty recombination centres and the electron life time increases [7].

The electron life time increment can alternatively be explained by means of the surface recombination velocity through the surface depletion zones via interband transitions [12]. In particular, when incident photons are absorbed, pairs of conjugate photocarriers are created within the surface depletion zone. The transfer of photoelectrons from an energy band (level) leaves their partner photoholes confined at the semiconductor surface. These photo-generated carriers increase the electron lifetime.

4. Conclusions

In this work, we have studied the dark and photocurrent properties of In_6S_7 crystals grown by the Bridgman method in the temperature regions of 170–300 and 150–300 K, respectively. The dark electrical resistivity analysis has shown that the crystals exhibit intrinsic-type conduction. The data allowed the determination of the energy band gap as 0.75 eV. In contrast to this property, the photocurrent analysis revealed the existence of two photoconductivity energy levels as 0.21 and 0.10 eV, being dominant at low and high temperatures, respectively. The photocurrent increases upon temperature increment up to a maximum temperature of 230 K, and thereafter decreases. The illumination intensity dependence of the photocurrent was found to exhibit supralinear, linear and approximately sublinear characters in the studied different temperature regions. These features are indications of a change in recombination mechanism, which is attributed to the exchange of the roles of trapping and recombination centres present in the crystals band gap. In addition, the crystals are found to exhibit photovoltaic properties. The maximum open-circuit photovoltage and maximum short-circuit current density were found to be 0.12 V and 0.38 mA cm^{-2}, respectively. These parameters are promising for the usage of these crystals as solar cells.

Acknowledgment

The authors express their thanks to the Semiconductors Laboratory technician Mr I Aydemir for his unlimited help through this work.

References

[1] Gavaleshko N P, Kitsa M S, Savchuk A I and Simchuk R N 1980 *Sov. Phys.—Semicond.* **14** 822
[2] Ansell H G and Boorman R S 1971 *J. Electrochem. Soc. Solid State Sci.* **118** 133
[3] Vinogradov E A, Gakhramanov N F, Dzhavadov B M and Tagirov V I 1980 *Sov. Phys.—Solid State* **22** 1661
[4] Gasanly N M, Dzhavadov B M, Ragimov A S, Tagirov V I and Guseinov R E 1981 *Phys. Status Solidi* b **106** K47
[5] Tagirov V I, Ismailov I M and Khusein A K 1978 *Sov. Phys.—Semicond.* **12** 1205
[6] Gamal G A 1997 *Semicond. Sci. Technol.* **12** 1106
[7] Bube R H 1992 *Photoelectronic Properties of Semiconductors* (Cambridge: Cambridge University Press) pp 59, 72, 83
[8] Osman M A 2000 *Physica* B **275** 351
[9] Qasrawi A F and Gasanly N M 2003 *Phys. Status Solidi* a **199** 277
[10] Tena-Zaera R, Katty A, Bastide S, Levy-Clement C, O'Regan B and Munoz-Sanjose V 2005 *Thin Solid Films* **483** 372
[11] Gordillo G and Calderon C 2003 *Sol. Energy Mater. Sol. Cells* **77** 163
[12] Anagnostakis E A 1994 *Phys. Status Solidi* a **146** K9